Compact and extended structure in B2 radio sources of intermediate strength

Padrielli, L.; Kapahi, V.K.; Katgert-Merkelijn, J.K.

ASTRONOMY & ASTROPHYSICS
SUPPLEMENT SERIES

DECEMBER **1981**, PAGE 473

Astron. Astrophys. Suppl. Ser. **46**, 473-481 (1981)

Compact and extended structure in B2 radio sources of intermediate strength

L. Padrielli, V. K. Kapahi (*) and J. K. Katgert-Merkelijn (**)

Laboratorio di Radioastronomia CNR, Istituto di Fisica, via Irnerio 46, Bologna 40126, Italia
(*) T.I.F.R. Centre, India Institute of Science Campus, Bangalore, 560012, India
(**) Sterrewacht, Postbus 9513, 2300 RA Leiden, Nederland

Received January 19, accepted April 6, 1981

Summary. — A complete sample of sources for which high-resolution data obtained at Jodrell Bank at 408 MHz are available has been observed with the Westerbork Synthesis Radio Telescope (WSRT) at 5 GHz. A catalogue of positions, structures and flux densities as derived from the WSRT observations is given, together with the results of an optical identification programme. A comparison of the high-resolution (i.e. up to 0.3 arcsec) data and the WSRT data (with a resolution of ≲ 8 arcsec) shows that :
a) The results at the different resolutions are generally in good agreement.
b) Approximately one half of the sources are resolved by the WSRT. One third of these have more than 10 % of their flux density at 408 MHz in bright unresolved features (< 1 arcsec).
c) One-third or more of sources not resolved by the WSRT are seen to be double in the Jodrell Bank data, implying a continuous range of linear sizes.
d) Of the sources not resolved with the WSRT a high percentage of galaxies and empty fields is found to have steep spectral indices.

Key words : Radio sources — structures — optical identifications — hot spots.

1. **Introduction.** — The statistical investigation of the structure of radio sources is an important tool of observational cosmology and for testing models of radio sources. Several authors have investigated the dependence of the angular size on the red shift z and have found clear evidence for the evolution of the linear source diameter with epoch in complete samples of quasars (Wardle and Miley, 1974) and in complete samples of radio galaxies (Katgert *et al.*, 1980). The same result was obtained by Kapahi (1975) from an analysis of the correlation between flux density and angular size. These studies were generally carried out with radio observations obtained with intermediate resolution instruments (about 10 arcsec) which give information on the extended structures of the radio sources on scales larger than tens of kpc.

Complete samples at various flux density limits were observed at 408 MHz at Jodrell Bank (JB) with an interferometer with a maximum resolution of ca. 0.3 arcsec in order to extend the statistical analyses for compact components of sources. Within this project Speed (1976) has obtained observations of very weak radio sources from the 5C2 and 5C3 catalogues. Also, Warwick (1977) has observed a sample of B2 sources (Colla *et al.*, 1970) selected at an intermediate flux density level (ca. 1 Jy at 408 MHz). We have observed the latter sample with the Westerbork Synthesis Radio Telescope (WSRT) at 5 GHz. Our aim was to compare the morphological properties observed with the WSRT, corresponding to sizes above tens of kpc with those obtained from the JB fringe visibility, which gives information below a few kpc.

The complete sample consists of 52 sources from the B2.1 catalogue with 29°18′ < Dec < 34°00′ and 23^h30^m < RA < 2^h30^m and flux densities in the range $0.9 \leq S_{408} < 2.5$ Jy. Although optical candidates had already been obtained by Grueff and Vigotti (1973), the identification procedure was repeated using the new, more accurate radio positions presented in this paper.

2. **Radio observations and reduction.** — The observations were made with the WSRT at 5 GHz. They consisted of three short measurements for a minimum of 5 minutes each at three widely spaced hour angles (generally 0^h and ± 4^h). The calibrated data were Fourier transformed to produce a two-dimensional map 2′ by 4′ in size. A Clean and Restore ([1]) technique (Högbom, 1974) was applied to remove the effect of side-lobe responses from the map. The results were compared with those of one-dimensional Fourier transforms to check their plausibility.

The 5σ level in the maps is about 25 mJy and this is the adopted limit above which we have generally considered a point-like subcomponent to be a true detection. The flux densities as obtained from the two-dimensional maps were compared with the total flux density in the field as derived from the visibility function ; the probability of finding a second unrelated source in the field of view is extremely small. For most sources the two values agree

([1]) The restoring beam is a gaussian function of (6 × 6/sin δ) arcsec² half power width corresponding to the resolution of a 12^h WSRT synthesis.

very well. The positions (of both the centroid of the sources and the individual components) are thought to be accurate to ~ 1 arcsec in right ascension and to ~ 2 arcsec in declination, for point sources.

Out of the 52 sources in the complete sample, 7 had already been observed by Fanti and Padrielli (1977), 4 by Grueff *et al.* (private communication) and 1 by Fanti *et al.* (1977), at 5 GHz using the WSRT. The data for these sources are directly comparable to those observed by us, as observation and reduction procedures were the same in all cases. Among the new observations, one source (0227 + 32) was not detected, probably because it is so extended that it is completely resolved at 5 GHz. Two sources (0003 + 31A, 0110 + 29) were not observed and for these WSRT structure information is lacking.

The 5 GHz date are listed in table I. One source (2351 + 32), included in the original observing list but not a member of the complete sample, is also included in the catalogue. Figure 1 shows the contour maps at 5 GHz of those sources which are extended by more than 10 arcsec and have been observed in the present programme (see the references quoted above for the sources already observed).

3. **Optical identifications.** — Optical identifications were made from the Palomar Sky Survey (PSS) prints. The positions of the optical candidates were measured to an accuracy of 1 arcsec. Since the radio positions have about the same accuracy only positional agreement need be used as a criterion for an optical identification. The adopted criteria are as follows : for single-component sources, objects are acceptable as identifications when the positional discrepancy is no greater than 4 arcsec in Right Ascension and 6 arcsec in Declination (approximate 3σ conditions). For sources with more than one component, identifications are accepted for each component as for single-component sources and for the sources as a whole in a strip of ± 4 arcsec along the line joining the outermost components.

The identifications are classed as follows : G = galaxy, B.O. = Blue stellar Object (candidate quasar) ; R.O. = Red stellar Object ; E.F. = empty field. The magnitudes have been obtained through comparison with star samples from selected area 57 (Stebbins *et al.*, 1950, Baum, 1963) for stellar objects and through comparison with galaxies of known photometry (Sandage, 1972) for galaxies. The accuracy of the estimate is about 0.5 m.

The identification procedure was the same as that used previously by the Bologna group, and the results are therefore directly comparable.

For the newly observed sources a comparison between the identifications and the number of background objects has been made for different radio structures in order to estimate the degree of contamination in this sample. The results are summarized in table II.

The number of spurious identifications was evaluated from the background counts given by Fanti and Padrielli (1977). An inspection of the data shows that the two identifications with the red objects could be spurious ; we also expect one spurious identification of an extended source with a blue object.

The identifications are listed in table I, where the optical positions of the objects are also given. Finding charts are given in figure 2.

The identification content of the sample is as follows :

E.F. + R.O.	: 30 (59 ± 11 %)
B.O.	: 13 (25 ± 7 %)
G	: 9 (18 ± 6 %) .

4. **Angular size distribution.** — Of the sample, 28 sources are extended or have more than one component ($\theta \geq 6$ arcsec) and 26 sources are unresolved at the resolution of the WSRT ($\theta < 6$ arcsec). For the two unobserved sources structure information has been taken from the JB data (Warwick, 1977) for 0003 + 31A and from Potash and Wardle (1979) for 0110 + 29. To the source 0227 + 32, undetected at 5 GHz (and also in the JB observations) an angular size larger than 20 arcsec has been assigned. Optical identifications in the two classes are distributed as given in table III. Figure 3 shows the distributions of the largest angular size for the three classes of objects. A large fraction of galaxies is seen to have an angular size > 20 arcsec. The E.F. and B.O. distribution are very similar at each other.

The distribution of the largest angular sizes for the sources of the whole sample gives a point on the $\log S - \log \theta$ relation studied by Swarup (1975). The value is $\theta_{\text{median}} = 9^{+4}_{-3}$ arcsec for fluxes with $S_{408} \sim 1$ Jy (at 408 MHz). This value may be underestimated due to possible incompleteness in the WSRT 5 GHz observations : at these low flux density levels components of double sources may have been missed when the flux ratio of the components differs considerably from unity. From the cumulative flux ratio distribution of observed doubles in the sample we calculate that we may have misclassified up to three double sources as point sources, one component being below our flux density limit. However, the value of θ_{median} we have found is in good agreement with the data obtained by Swarup (1975) at this flux level from an independent sample selected at 327 MHz.

In the following discussion the angular sizes have on occasion been transformed into linear sizes, using either a red shift estimated from the magnitudes for G sources, or assuming $z = 0.5$, $q_0 = 0$, $H_0 = 100$ km/s/Mpc for E.F. sources and B.O. sources.

5. **Comparison with the Jodrell Bank data.** — 5.1 RESOLVED SOURCES. — Out of 26 extended sources with structure information, we have found 20 simple doubles, 3 triples, 1 complex, and 2 slightly resolved sources. Figure 4 presents a comparison between angular sizes derived from JB data and the 5 GHz data for the sources with WSRT size $\theta > 6$ arcsec. In figure 4a θ_{JB} is plotted as a function of θ_{W} for the sources detected at JB and figure 4b shows the distribution of WSRT angular size for the sources not detected at JB. The agreement between the WSRT morphology and that of JB (when detected) is good for 7 of the 10 double sources. The three discordant cases are the sources 0153 + 29, 0200 + 30, 2335 + 30, seen as asymmetric doubles at WSRT and as single at JB (see Fig. 1).

There are two possible explanations :

1) the source detected at JB coincides with the nuclear component of a triple source of which one outer component is below the WSRT noise level (possibly 0200 + 30, which has a spectral index of 0.22) ;

2) the JB source represents a hot spot of one component of a double source ; the second component either does not contain compact features or is too weak.

Furthermore, some sources can be not true doubles but superpositions of single sources. However as can be derived from the 6 cm source counts (Willis and Miley, 1979), the probability of finding chance coincidences in the present sample is vanishingly small.

There are no optical identifications to help us distinguish between the various possibilities.

In the following discussion these sources have been classed as resolved.

Of the three triple sources only 2348 + 30 was not detected at JB ; in the case of 0055 + 30 only the nucleus was seen at JB and 0110 + 29 was detected at JB as a double source, one component coinciding with the nucleus and the second one with the stronger of the two outer components (Potash and Wardle, 1979).

Figure 6 shows the maximum fringe visibility γ_{max} measured at JB *versus* the component-separation for the double and slightly resolved sources. Also drawn in are the predicted relations for various source morphologies based on 3C33, Cygnus A (Warwick, 1977), 3C382 and 3C449 (Fanti *et al.*, 1977, and private communication). These relations were derived by calculating the expected observational parameters for these sources as a function of distance. The figure suggests that most of the double sources in the sample have morphological properties typical of high-luminosity sources, i.e. compact bright features at the outer edges of the radio lobes (Fanaroff and Riley, 1974). However, the values for a number of sources (20-25 % of the sample) are indicative of structures like those of 3C382 and 3C449. These are galaxies with a radio power at 408 MHz in the range $24.5 < \log P < 25.5$ and with one bright (3C382), or two weak *hot spots* (3C449).

Figure 7 gives a plot of the JB maximum fringe visibility against spectral index for the double sources ; the three classes have been indicated by different symbols.

Detection at JB indicated that (part of) the radio emission is concentrated in small size regions ($\leqslant$ 0.5 arcsec) or *hot spots*. For those resolved sources for which $\alpha > 0.60$ we have 5/11 detections for empty-field sources, 1/5 for galaxies and 2/5 for B.O.'s. Hot spots in the nearer galaxies could have been resolved out by the JB resolution.

5.2 COMPACT SOURCES ($\theta < 6''$). — Of the 24 sources not resolved in the Westerbork observations 5 were not detected at JB (0032 + 30, 0125 + 32, 2330 + 30, 2355 + 31, 2359 + 31). Figure 5 gives the angular size distribution for the sources detected at JB. Among these, 8 sources are double and 11 are single with an angular diameter < 1 arcsec. Generally the JB morphology is in good agreement with the WSRT limits. The 5 sources undetected at JB are all empty-field sources with steep spectral indices (α(408-5000) $\geqslant$ 0.90) where α is defined such that $S_\nu \propto \nu^{-\alpha}$.

Figure 8 corresponds to figure 7, but for unresolved objects. Inspecting this figure together with figure 7 the following points can be noted : there are the obvious and well-known characteristics : unresolved sources have a higher percentage of flat spectrum objects (mostly B.O.), indicating domination at 5 GHz by self-absorbed nuclei.

It is however remarkable that a large fraction of unresolved sources that are either unidentified or identified with faint galaxies have very steep spectral indices and high values of γ_{JB} (e.g. 2330 + 29 has $\alpha = 0.95$, $\gamma_{JB} = 1.07$). These sources may be compact doubles without a dominant self-absorbed nuclear component but with steep spectrum unresolved features in the radio lobes ($\theta \leqslant 0.3''$ or linear sizes of less than 2 kpc). They would be interesting objects for VLBI.

Finally we want to discuss the already mentioned 5 sources (4 E.F.s and 1 R.O.) not detected at JB. All these sources have $\alpha > 0.9$. They could consist of flat-spectrum cores with very steep spectrum halos. A spectral index flatter than 0.5 for the component seen at WSRT is enough to give a flux density at 408 MHz below the JB detection limit. However, we have found only one source with a spectral index flatter than 0.5 among the 14 E.F. sources detected at JB. It is also know that empty field sources dot not generally have strong nuclear components (e.g. Longair, 1975). It therefore appears more probable that the above sources actually have double or extended structure smaller than 6 arcsec (< 50 kpc) and component diameters of $\gtrsim$ 1 arcsec (ca. 4 kpc) ; these sources with low maximum fringe visibility would have a very small percentage of flux density in the hot spots (< 10 to 20 %) compared to the models shown in Figure 6.

6. **Conclusions.** — We can summarize the results obtained here as follows :

a) The WSRT observations show source structure with linear sizes larger than ca. 50 kpc in about half of the cases, assuming $z > 0.5$ for E.F. and B.O. sources. One-third of these extended sources have more than 10 % of their flux density at 408 MHz in bright features of linear intrinsic size $\lesssim$ 2-3 kpc, similar to the hot spots of Cygnus A.

b) For the sources not resolved in the WSRT observations JB measurements indicate that one-third or more are compact doubles.

Furthermore, only 4 out of 11 sources seen as single at JB (ca. 1″) show a spectral index flatter than 0.5, probably due to a compact self-absorbed dominant component. Therefore, as expected due to the low-frequency selection, the high-resolution measurements at 408 MHz refer mostly to outer *hot spots,* even in structures with separations less than a few kpc.

c) We have found a high percentage of steep-spectral-index sources with high JB maximum fringe visibility associated with empty fields or faint galaxies.

d) Finally, the *largest angular size* distribution of the whole sample provides a point on the log S $-$ θ relation that is in good agreement with the relation found by

Swarup (1975). This relation was interpreted by Kapahi (1975) in terms of evolution of the intrinsic diameter of sources.

Acknowledgements. — We thank the Staff of the WSRT for carrying out the observations, and the reduction staff in Leiden for calibrating the data. Unpublished data were kindly contributed by Dr. Grueff. We are grafetul to Dr. R. Fanti and Dr. G. K. Miley for critical reading of the manuscript, and Dr. Veron for many useful comments.

The Westerbork Synthesis Radio Telescope is operated by the Netherlands Foundation for Radio Astronomy with the financial support of the Netherlands Organization for the Advancement of Pure Research (ZWO).

References

BAUM, W. : 1963, unpublished data.
BOZYAN, E. P. : 1979, *Astron. J.* **84**, 910.
COLLA, G., FANTI, C., FANTI, R., FICARRA, A., FORMIGGINI, L., GANDOLFI, E., GRUEFF, G., LARI, C., PADRIELLI, L., ROFFI, G., TOMASI, P., VIGOTTI, M. : 1970, *Astron. Astrophys. Suppl. Ser.* **1**, 281.
EDWARDS, T., KROMBERG, P. P., MENARDI, G. : 1975, *Astrophys. J.* **80**, 1005.
FANAROFF, B. L., RILEY, J. M. : 1974, *Mon. Not. Roy. Astron. Soc.* **167**, 31P.
FANTI, R., PADRIELLI, L. : 1977, *Astron. Astrophys. Suppl. Ser.* **29**, 263.
FANTI, C., FANTI, R., GIOIA, I. M., LARI, C., PARMA, P., ULRICH, M. H. : 1977, *Astron. Astrophys. Suppl. Ser.* **29**, 279.
GRUEFF, G., VIGOTTI, M. : 1973, *Astron. Astrophys. Suppl. Ser.* **11**, 41.
GRUEFF, G., VIGOTTI, M., SPINRAD, H. : 1980, *Astron. Astrophys.* **86**, 50.
HARRIS, D. E., LARI, C., VALEÉ, J. P., WILSON, A. S. : 1980, *Astron. Astrophys. Suppl. Ser.* **42**, 19.
HAZARD, C., JAUNCEY, D. L., BACKER, D. C. : 1970, *Astron. J.* **75**, 1039.
HEWITT, A., BURBIDGE, G. : 1980, *Astrophys. J. Suppl.* **43**, 57.
HÖGBOM, J. A. : 1974, *Astron. Astrophys. Suppl.* **15**, 417.
KAPAHI, V. K. : 1975, *Mon. Not. Roy. Astron. Soc.* **172**, 513.
KATGERT-MERKELIJN, J. K., LARI, C., PADRIELLI, L. : 1980, *Astron. Astrophys. Suppl. Ser.* **40**, 91.
LONGAIR, M. S. : 1975, *Mon. Not. Roy. Astron. Soc.* **173**, 309.
OLSEN, E. T. : 1970, *Astron. J.* **75**, 764.
POTASH, R. I., WARDLE, J. F. C. : 1979, *Astron. J.* **84**, 707.
POTASH, R. I., WARDLE, J. F. C. : 1980, *Astrophys. J.* **239**, 42.
RUDNICK, L., ADAMS, M. T. : 1979, *Astron. J.* **84**, 437.
SANDAGE, A. : 1972, *Astrophys. J.* **178**, 25.
SARGENT, W. L. W. : 1973, *Astrophys. J.* **182**, L13.
SCHMIDT, M. : 1975, *Astrophys. J.* **195**, 253.
SPEED, B. : 1976, *Mon. Not. Roy. Astron. Soc.* **177**, 137.
STEBBINS, J., WITHFORD, A. E., JOHNSON, M. L. : 1950, *Astrophys. J.* **112**, 469.
SWARUP, G. : 1975, *Mon. Not. Roy. Astron. Soc.* **172**, 501.
ULRICH, M. H. : 1976, *Astrophys. J.* **206**, 364.
WARDLE, J. F. C., MILEY, G. K. : 1974, *Astron. Astrophys.* **30**, 305.
WARWICK, R. S. : 1977, *Mon. Not. Roy. Astron. Soc.* **179**, 1.
WILLIS, A. G., MILEY, G. K. : 1979, *Astron. Astrophys.* **76**, 65.
WILLS, B. J. : 1976, *Astrophys. J.* **81**, 1031.
VERON, M. P., VERON, P., ADGIE, R. L., GENT, H. : 1976, *Astron. Astrophys.* **47**, 1401.

TABLE I. — *Sources catalogue.*

The data are listed as follows :

Column 1 : B2 name.

Columns 2 and 3 : Right Ascension and Declination (epoch 1950.0) of the centroid of the radio emission or of the optical object. A, B and C mark different components of the same radio source. OP indicates the position of the optical identification.

Columns 4 and 5 : Flux density at 408 MHz in mJy, taken from the B2 catalogue. The fraction γ of the flux density observed at Jodrell Bank is given in parentheses. For most of the sources this value is equivalent to the maximum observed fringe visibility (Warwick, 1977).

Columns 6 and 7 : 5 GHz density of each component and for the whole source (column 7). The total flux density can be larger than the sum of the flux densities of the components when there is extended low brightness structure.

Columns 8 and 9 : Angular size (θ) per component in arcsec (Gaussian model). In parentheses position angle in degrees, from north through east.

Column 10 : Largest angular size of source in arcsec.

Column 11 : Spectral index α(408-5000), defined such that $S_\nu \propto \nu^{-\alpha}$.

Columns 12 and 13 : Optical Identification as follows : BO = Blue stellar Object, RO = Red stellar Object, G = Galaxy, E = Empty field. The photographic magnitude (for BO) and the visual magnitude (for G and RO) is given in parentheses.

Column 14 : An asterisk indicates reference to footnotes for further information.

Notes to table I.

0003+31A No 5 GHz WSRT observations. Optical identification taken from Grueff and Vigotti (1973).

0007+33 5 GHz WSRT data taken from Fanti and Padrielli (1975). Observations at 2.7 and 8.1 GHz are reported by Potash and Wardle (1979). The suggested identification is a QSO (z = 0.743) (Hewitt and Burbidge, 1980).

0008+32 5 GHz WSRT data obtained by Grueff (private communication). Identification and finding chart already published by Ulrich (1976) (z = 0.107).

0013+32A Bozyan (1979) has already classified the field as empty.

0014+31A The same identification was already proposed by Wills (1976) who gives the finding chart.

0032+30 5 GHz WSRT data obtained by Grueff (private communication). The new, more accurate radio position does not confirm the previous identifications with galaxies of this source (Bozyan, 1979 ; Grueff *et al.*, 1980).

0051+31 Optical object confused by nearby 17th mag. blue star.

0055+30 5 GHz WSRT data and identification taken from Fanti *et al.* (1977).

0110+31 The suggested identification is a QSO (z = 0.603) (Hewitt and Burbidge, 1980). Finding chart published by Edwards *et al.* (1975).

0110+33 5 GHz WSRT data and optical identification taken from Fanti and Padrielli (1977).

0110+29 Observations at 2.7 and 8.1 MHz are reported by Potash and Wardle (1979). The source is triple with a largest angular size of 77 arcsec. The suggested identification is a QSO (z = 0.363) (Hewitt and Burbidge, 1980).

0125+33 5 GHz WSRT data and optical identification taken from Fanti and Padrielli (1977).

0138+29B Finding chart published by Wills (1976), who proposed the same identifications.

0149+33 The suggested identification is a QSO (z = 2.431) (Hewitt and Burbidge, 1980). 5 GHz WSRT data taken from Fanti and Padrielli (1977).

0154+31A The suggested identification is QSO (z = 0.373) (Hewitt and Burbidge, 1980). Finding chart published by Veron *et al.* (1976).

0154+31B 5 GHz WSRT data by Grueff (private communication). Identifications and finding chart already published by Ulrich (1976). The galaxy is in the Abell cluster A 278 (Harris *et al.*, 1980).

0157+33 The new ratio position does not confirm previous identifications with blue object : Olsen (1970), Hazard *et al.* (1980). Furthermore, Schmidt (1975) took a spectrum of this Blue object and concluded that it is possibly a star. The new identification is a very faint object at the limit of the PSS.

0202+31 The suggested identification is a QSO (z = 1.466) (Hewitt and Burbidge, 1980). Finding chart published by Wills (1976).

0204+32 Finding chart published by Hazard *et al.* (1970).

0206+33, 0216+33B } 5 GHz WSRT data and optical identification taken from Fanti and Padrielli (1977).

0227+32 Source undetected in the 5 GHz WSRT observations. Optical identification by Grueff and Vigotti (1973). Also Bozyan (1979) has classified the field as empty.

2330+30 Rudnick and Adams (1979) have already classified the field as empty.

2342+29 Finding chart published by Olsen (1970). Sargent (1973) has measured the redshift of the galaxy (z = 0.131).

2347+30 5 GHz WSRT data by Grueff (private communication). Identification and finding chart by Grueff *et al.* (1980).

2349+32B Interesting structure (see Fig. 1). Observations at 5 GHz are reported by Potash and Wardle (1980). The suggested identification is a QSO (z = 0.659) (Hewitt and Burbidge, 1980).

2351+32 Not in complete sample (not observed at JB).

TABLE I.

B2 NAME		R.A. 1950	DEC. 1950	S 408 TOT	JBν	S 5000 COM	S 5000 TOT	θ(P.A.)	LAS	α	OPT. ID.	
0003+31A				1170	(0.84)			<6			E	*
0003+31B		00 03 21.14	31 23 07.1	1760	(0.75)	243	260			0.76	E	
0007+30		00 07 32.80	30 28 37.2	1030	(<0.1)	66	125	15(170) 7(80)		0.84	E	
0007+33	A	00 07 50.10	33 13 31.7	1660	(0.12)	107		12	75	0.96		*
	B	49.90	12 17.0			74		13				
	OP	50.06	12 55.4								BO(19.5)	
0008+32	A	00 08 36.9	32 01 14.	1150	(<0.1)	91		37	294	0.86		*
	B	55.5	31 58 20.			(26)		10				
	OP	43.6	32 00 33								G(16.5)	
0013+32A	A	00 13 36.98	32 21 56.3	1840	(<0.2)	72	160	5(107)	54	0.97	E	*
	B	34.63	22 41.8			67		8(45)				
0013+32B		00 13 53.17	32 43 19.1	1020	(0.40)	65		<6		1.10	E	
0014+31A	A	00 14 25.22	31 52 35.0	1210	(<0.2)	61	130	10(12)	17	0.89		*
	B	26.16	47.4			35		7(80)				
	OP	25.42	42.7								BO(18.8)	
0015+30B	A	00 15 54.83	30 49 34.4	1040	(<0.1)	46	100	6(24)	49	0.93		
	B	54.71	48 45.5			32		<6				
	OP	54.62	49 21.4								RO(17.0)	
0024+32B		00 24 29.15	32 30 00.7	1170	(0.80)	70		<6		1.12	E	
0032+30		00 32 05.7	30 09 26.	1040	(<0.2)	43		<6		0.98	E	*
0039+32	A	00 39 05.99	32 08 22.0	2200	(0.20)	150		<6	32	0.94		
	B	03.67	33.7			60						
	OP	04.94	27.3								G(20)	
0039+29B	A	00 39 59.27	29 49 37.9	990	(<0.1)	57	100		12	0.91	E	
	B	58.65	30.9			41						
0044+30		00 44 25.05	30 11 23.1	1960	(0.21)	109	122	<6		1.11	E	
0051+30A	A	00 51 07.29	30 58 38.1	1960	(0.50)	99		<6	16	1.03	E	
	B	06.29	27.8			50		<6				
0051+31		00 51 34.34	31 44 52.8	1430	(0.61)	160		<6		0.87		*
	OP	34.53	49.3								G?(18)	
0055+30	A	00 55 05.7	30 04 57.	1960	(0.17)	670			48	-0.02		*
	B	02.7	05 25.			500						
	C	16.0	03 00.			10						
	OP	05.6	04 56.								G(11.3)	
0055+31A		00 55 22.49	31 05 01.9	1320	(0.60)	186		<6		0.78	E	
0055+31B		00 55 37.27	31 29 42.5	1240	(0.86)	150		<4		0.84		
	OP	37.22	42.0								G(20)	
0110+31		01 10 03.76	31 52 23.6	1420	(0.64)	615		<4		0.33		*
	OP	03.70	23.2								BO(17.4)	
0110+33		01 10 06.44	33 35 12 6	980	(0.76)	90		<6		0.90	E	*
0110+29				1670	(0.15)						BO(16.4)	*
0125+32		01 25 10.64	32 29 02.0	2310	(<0.2)	82		<6		1.33		
	OP	10.83	00.9								RO(16.8)	
0125+33		01 25 21.74	33 09 02.2	1560	(0.49)	320		<3		0.62	E	*
0138+29B		01 38 38.05	29 27 29.6	1360	(<0.1)	155		10(93)		0.87		*
	OP	37.89	30.3								BO(18.3)	
0149+33		01 49 40.02	33 35 47.5	1310	(0.95)	565		<3		0.25		*
	OP	39.94	46 4								BO(19.0)	
0153+30	A	01 53 04.18	30 01 46.8	1080	(0.25)	45			14	1.02	E	
	B	04.97	38.9			39						
0153+29	A	01 53 05.44	29 41 03.1	1290	(0.13)	85	155	<6	13	0.85	E	
	B	06.27	10.1			34		<6				
0154+31A		01 54 21.49	31 39 39.3	2420	(0.60)	395		<4		0.72		*
	OP	21.56	43.1								BO(18.3)	
0154+31B	A	01 54 22.2	31 59 48	1080	(<0.1)	49		12	35	1.09		*
	B	23.2	31 59 25			20		9				
	OP										G(15.5)	
0157+33	A	01 57 49.19	33 23 42.6	1240	(<0.2)	101	175	16(99) 9(189)	25	0.78		*
	B	51.20	45.6			59		6(95)				
	OP	50.58	46.7								G?(20)	
0200+30	A	02 00 51.54	30 27 06.0	930	(0.81)	405	560	<4	69	0.20	E	
	B	50.42	28 13.4			98		7(177)				
0202+31		02 02 09.66	31 58 11.4	1050	(0.74)	500		<3		-0.14		*
	OP	09.58	10.5								BO(16.3)	
0204+32		02 04 00.37	32 47 11.7	2000	(0.90)	247		<4		0.83		*
	OP	00.49	12.0								BO(18.0)	
0204+31		02 04 39.61	31 37 51.2	1380	(0.83)	424		<4		0.47		
	OP	39.56	53.0								BO(18.3)	
0206+33		02 06 39.08	33 40 09.9	1140	(<0.1)	145		9		0.84	E	*
0216+33B		02 16 49.69	33 34 36.1	1070	(0.60)	141		14		0.84	E	*
0217+32		02 17 49.88	32 27 22.9	1500	(0.76)	525		6(52)		0.42		
	OP	49.95	24.5								BO(17.6)	
0222+31C		02 22 19.29	31 05 26.2	910	(0.99)	522		<4		0.22	E	
0226+29	A	02 26 52.80	29 25 08.2	1440	(0.44)	95		<6	34	0.86		
	B	53.20	24 34.9			71		6(43)				
	OP	52.89	52.7								BO(19.4)	
0227+32				1120	(<0.1)	<30		>20			E	*
2330+29		23 30 34.87	29 37 13.6	1070	(1.07)	98		<6		0.95	E	
2330+30		23 30 34.95	30 38 47.3	1140	(<0.1)	70		5(59)		0.95	E	*
2335+30A	A	23 35 04.27	30 07 07.9	1340	(0.87)	142		<6	39	0.80	E	
	B	06.39	06 40.0			39						
2341+30	A	23 41 48.29	30 19 11.9	1100	(<0.1)	57			19	0.97	E	
	B	48.35	18 53.1			41						
2342+29		23 42 32.95	29 26 07.1	1590	(0.88)	273		<4		0.70		*
	OP	33.02	05.0								G(16.5)	
2346+30		23 46 02.72	30 29 01.2	980	(0.55)	168		<6		0.70	E	
2347+30	A	23 47 51.6	30 13 06	1010	(<0.1)	75		12	37	0.79		*
	B	53.7	31			65		21				
	OP	52.19	17.4								G(19.5)	
2348+30	A	23 48 33.63	30 03 25.7	1510	(<0.1)	60		24(179)	99	0.92	E	
	B	32.75	12.3			46		7(11)				
	C	28.91	02 08.2			46		10(6)				
2349+32B	A	23 49 48.56	32 47 35.0	2360	(<0.1)	194		30(8) 16(98)	51	0.93		*
	B	50.26	46 48.5			36						
	OP	47.92	47 49.1								G(19)	
	OP	48.94	18.2								BO(20.1)	
2351+32	A	23 51 39.79	32 38 42.4	3810	(-)	137		14(25)	41	1.09	E	*
	B	37.54	13.2			113		6(21)				
2355+31		23 55 40.28	31 13 21.3	1330	(<0.2)	77		<6		0.89	E	
2359+31		23 59 40.11	31 23 00.4	1000	(<0.2)	88		<6		0.97	E	

TABLE II. — *Identification content of the newly observed sources and number of spurious identifications expected.*

		B.O.	G	R.O.	E
single	id.	7	3	1	10
	sp.	0.2	0.1	0.6	
double or extended	id.	4	3	1	11
	sp.	0.8	0.3	1.5	

TABLE III. — *Optical identification content for resolved and unresolved sources.*

	E+R.O.	B.O.	G
resolved	14	6	6
unresolved	16	6	3

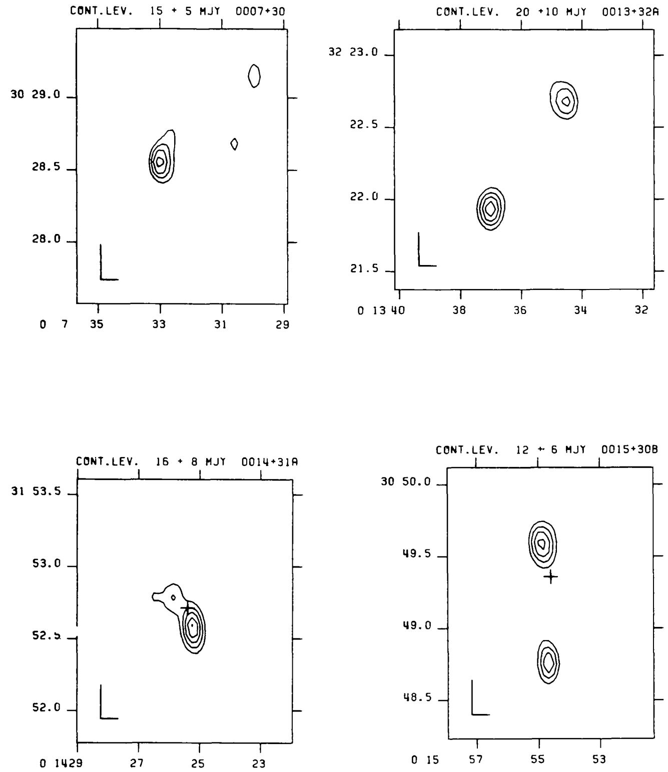

FIGURE 1 (1).

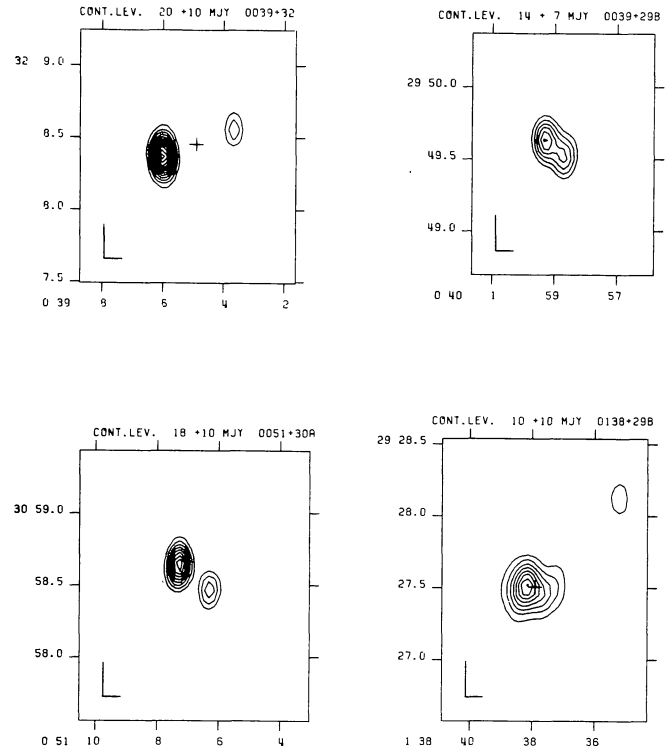

FIGURE 1 (2).

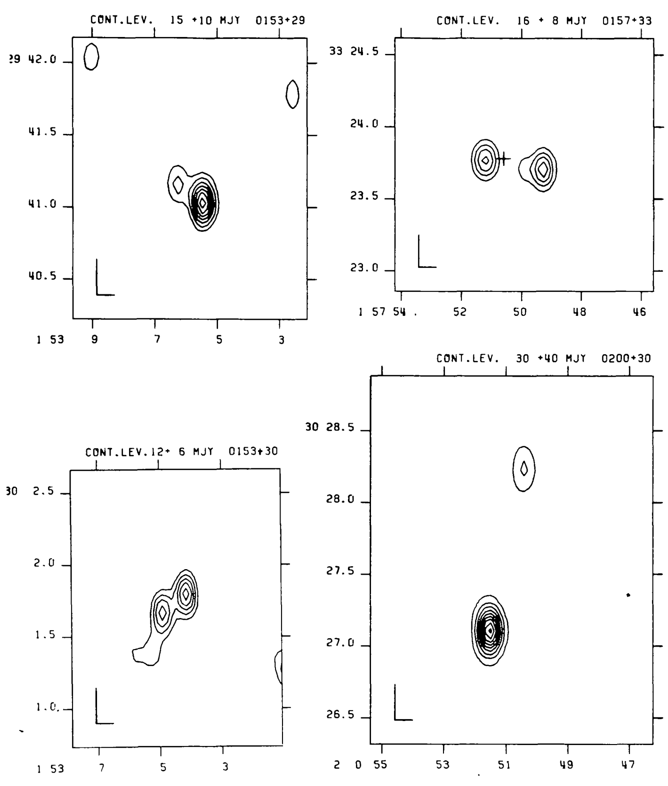

FIGURE 1 (3).

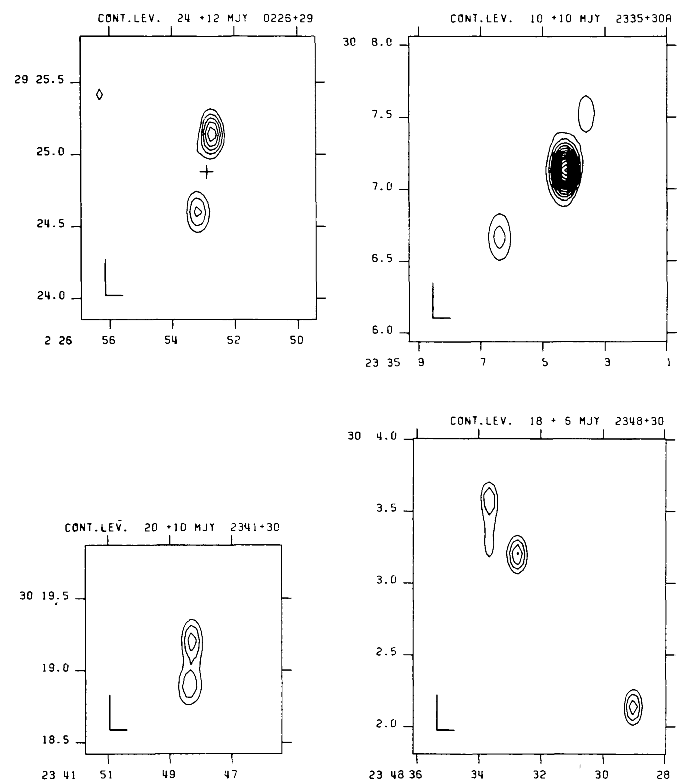

FIGURE 1 (4).

FIGURE 1. — 5 GHz contour maps for sources observed with the WSRT in the present programme. Source names and contour levels are indicated at the top of the diagrams. Positions of optical identifications are marked with a cross.

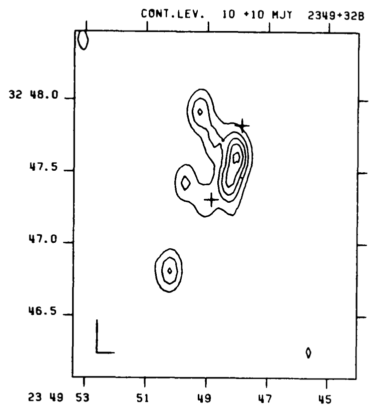

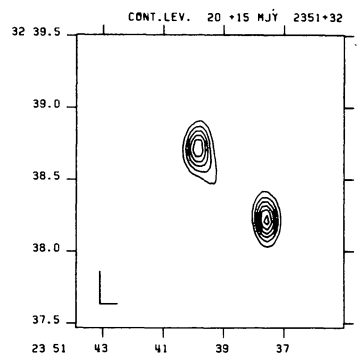

FIGURE 1 (5).

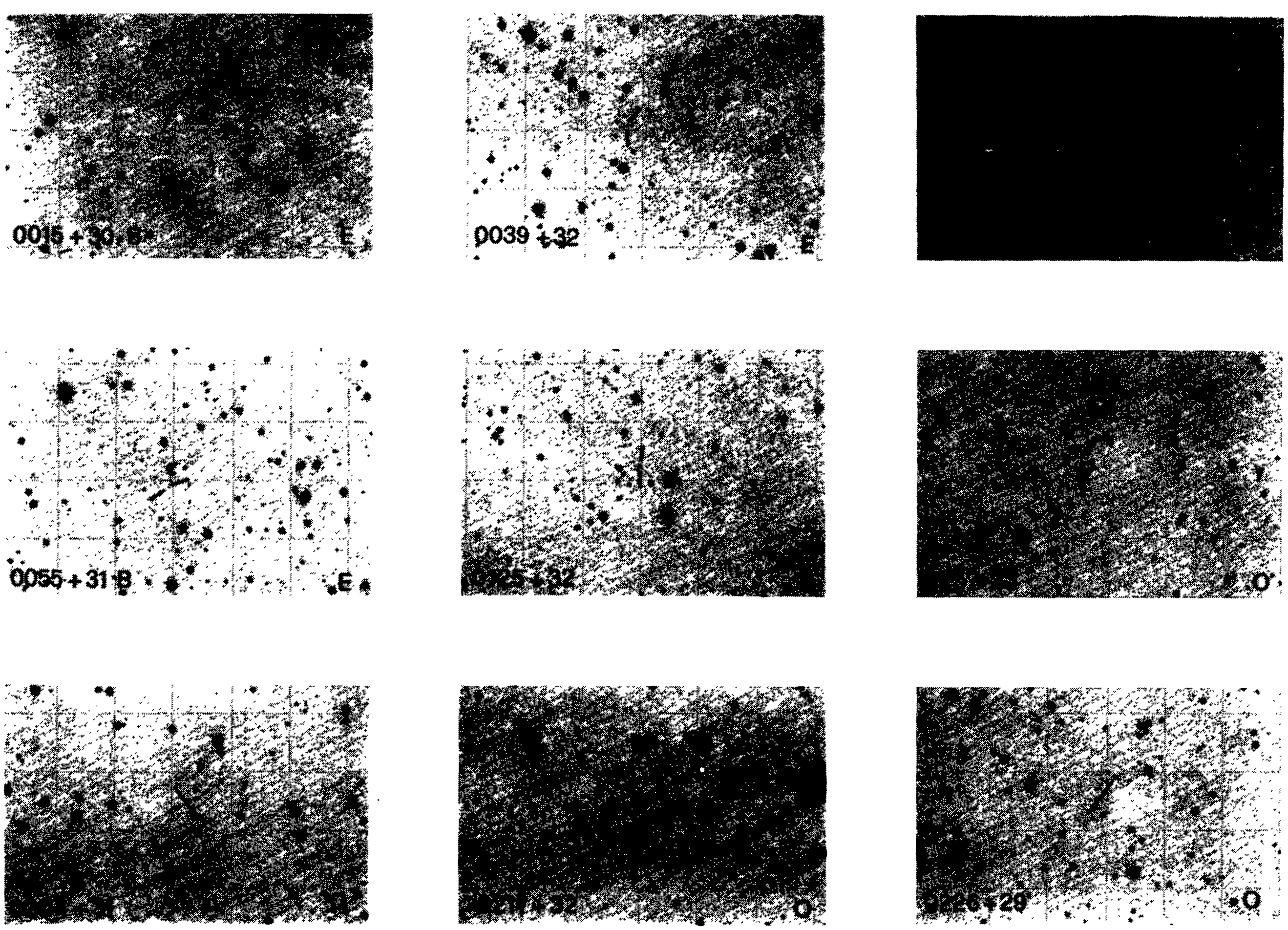

FIGURE 2. — Finding charts for new identifications. The scale is 1 mm = 12 arcsec. Finding charts for galaxies have been reproduced from the PSS red or « E » prints, for B.O.'s from the blue or « O » prints. Reproductions courtesy of National Geographic Society, Palomar Sky Survey.

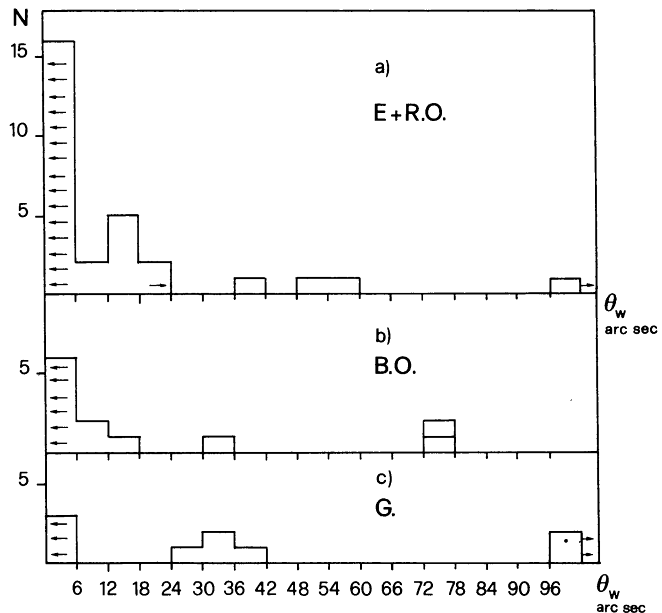

FIGURE 3. — Distribution of largest angular sizes for the three classes of objects.

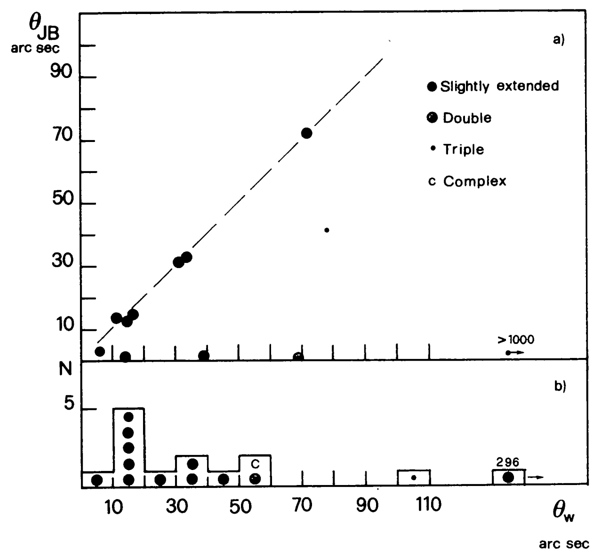

FIGURE 4. — Comparison between JB and WSRT angular sizes for sources with WSRT angular sizes larger than 6 arcsec.
a) JB angular size *versus* WSRT angular size for sources detected at JB.
b) WSRT angular size distribution for sources not detected at JB.

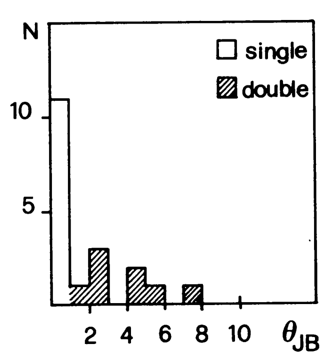

FIGURE 5. — JB angular size distribution for sources not resolved by the WSRT (θ < 6 arcsec).

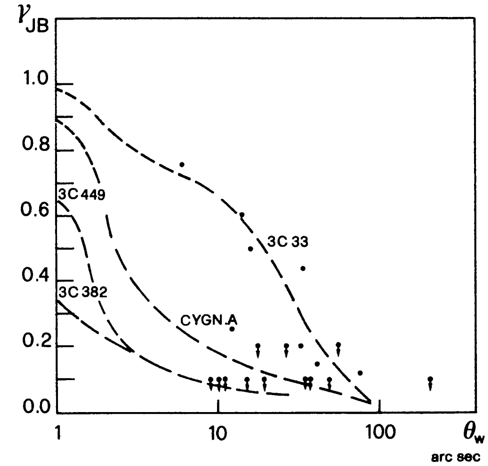

FIGURE 6. — The JB maximum fringe visibility γ_{max} *versus* component separation for sources with $\theta_w > 6$ arcsec. The dashed lines indicate predicted relations for various source morphologies, *viz.* : symmetrical hot spots (3C33 type), double hot spots in extended emission (Cyg A type), single bright hot spot (3C392 type), two weak hot spots (3C449 type).

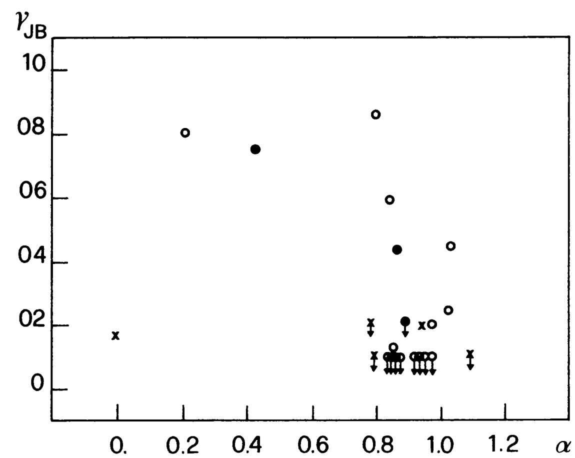

FIGURE 7. — JB fringe visibility (γ_{JB}) *versus* spectral index for sources resolved at the WSRT. Different classes are indicated as follows : ○ : Empty fields, ● : Blue objects, × : Galaxies.

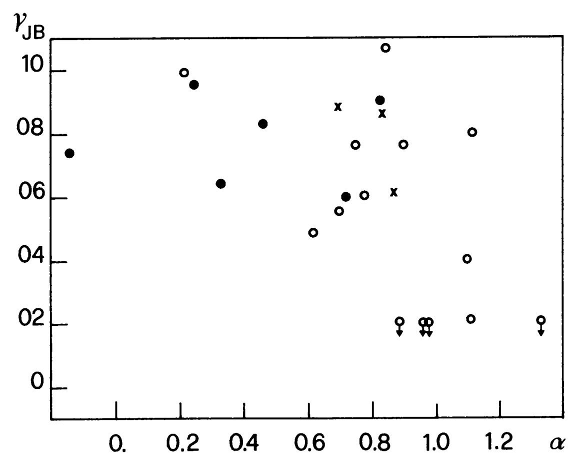

FIGURE 8. — As figure 7 but for sources unresolved with the WSRT.